Biosensors and Bioelectronics 35 (2012) 224–229

Contents lists available at SciVerse ScienceDirect

Biosensors and Bioelectronics

journal homepage: www.elsevier.com/locate/bios

Detection of p53 gene point mutation using sequence-specific molecularly imprinted PoPD electrode

Ashutosh Tiwari[a,b,c,*], Swapneel R. Deshpande[a], Hisatoshi Kobayashi[c,d], Anthony P.F. Turner[a,*]

[a] Biosensors and Bioelectronics Centre, Institute of Physics, Chemistry and Biology, IFM-Linköping University, S-58183 Linköping, Sweden
[b] Linköping Integrative Regenerative Medicine (IGEN) Centre, IKE-Linköping University, S-581 83 Linköping, Sweden
[c] International Center for Materials Nanoarchitectonics, National Institute for Materials Science, 1-2-1, Sengen, Tsukuba, Ibaraki 305 0047, Japan
[d] JSR-CREST, 5, Sanbancho, Chiyoda-ku, Tokyo 102-0075, Japan

ARTICLE INFO

Article history:
Received 13 February 2012
Accepted 25 February 2012
Available online 15 March 2012

Keywords:
Sequence-specific sensor
Genetic recognition
Molecularly imprinted polymer
Oligodeoxyribonucleotide imprinted electrode
Amperometric biosensor

ABSTRACT

An amperometric sequence-specific molecularly imprinted single-stranded oligodeoxyribonucleotide (ss-ODN) biosensor was fabricated and characterised in this study. Using ss-ODN as the template and *o*-phenylenediamine as the functional monomer, the ODN biosensor was fabricated by an electropolymerisation process on an indium-tin oxide (ITO) coated glass substrate. The template ss-ODN was washed out of the ss-ODN/poly(*o*-phenylenediamine)(PoPD)/ITO electrode using sterilised basic ethanol-water. The resulting ss-ODN imprinted PoPD/ITO electrode was characterised using Fourier transform infrared spectroscopy (FTIR), scanning electron microscopy (SEM) and cyclic voltammetry (CV). The amperometric responses, i.e., Δi as a function of the target ss-ODN concentration was studied. The biosensor using ss-ODN imprinted PoPD/ITO as the working electrode showed a linear Δ current response to the target ss-ODN concentration within the range of 0.01–300 fM. The biosensor showed a sensitivity of 0.62 μA/fM, with a response time of 14 s. The present novel molecularly imprinted ss-ODN biosensor could greatly benefit in terms of cost-effectiveness, storage stability, ultra sensitivity and selectivity together with the potential for improved commercial genetic sensors.

1. Introduction

The sequence of the nucleotide units in DNA plays an important role in the storage and transfer of genetic information in living systems (Bruce et al., 2002; Wolfram, 1984). Recently, DNA biosensors and gene chips have generated considerable interest for easy, rapid and inexpensive testing of genetic and infectious diseases (Liu and Bazan, 2005; Wang, 2000). Such devices intimately couple a specific type of DNA, serving as a biological recognition element, with optical, electrochemical or piezoelectric transducers to translate the genetic recognition event into a corresponding analytical signal. Electrochemical biosensors are emerging as excellent analytical tools for rapid and inexpensive genetic recognition (Kerman et al., 2004).

The conventional methods for the analysis of specific gene sequences are based on either direct sequencing or DNA hybridisation (Tiwari and Gong, 2009; Haupt and Mosbach, 2000). Because of its simplicity, DNA hybridisation is more commonly used in the diagnostic laboratory than the direct sequencing method. In DNA hybridisation, the target gene sequence is identified by a DNA probe that can form a double-stranded hybrid with its complementary nucleic acid, with high efficiency and extremely high specificity in the presence of a mixture of many different, non-complementary, nucleic acids. DNA probes are single-stranded oligonucleotides, labeled with either radioactive or non-radioactive material, to provide detectable signals for DNA hybridisation. Radioactive labels are extremely sensitive, but have the obvious disadvantage of short shelf life, potential risks associated with exposure of personnel to radiation, high cost and complexity associated with their storage and disposal. On the other hand, non-radioactive probes, such as enzymatic or luminescence labels, are less sensitive and flexible in terms of design and application. Therefore, large-scale, routine clinic screening based on gene diagnostics is limited by the currently available technologies.

In recent years, molecularly imprinted polymers (MIPs) have attracted much attention due to their multifarious potential applications including in sensors, separations, catalysis, drug delivery and waste management (Ramanaviciene and Ramanavicius, 2004; Parmpi and Kofinas, 2004; Slinchenko et al., 2004). To prepare MIPs, functional monomers are initially self-assembled around the template molecule via interaction between functional groups on both

* Corresponding authors at: Biosensors and Bioelectronics Centre, Institute of Physics, Chemistry and Biology, Linköping University, S-58183 Linköping, Sweden. Tel.: +46 1328 2395; fax: +46 1313 7568.
E-mail addresses: ashutosh.tiwari@liu.se, ashunpl@gmail.com (A. Tiwari), anthony.turner@liu.se (A.P.F. Turner).

0956-5663/$ – see front matter © 2012 Elsevier B.V. All rights reserved.
doi:10.1016/j.bios.2012.02.053

the template and the monomers. The self-assembled functional monomers are subsequently cross-linked. Thereafter, the template molecules are removed from the MIPs, thereby leaving behind cavities or imprinted-structures that can specifically recognise and rebind with the template molecules (Ansell et al., 1996). Hence, MIPs have the ability to mimic biological functions through their three-dimensional cavities with specific size, shape, and functionality for mimetic recognition of target molecules (Merkoci and Alegret, 2002; Piletsky et al., 2001; Mosbach, 1994) and have already been applied for interesting applications such as the separation and recognition of glucose (Wizeman and Kofinas, 2001), cholesterol (Whitcombe et al., 1995), hemoglobin (Shiomi et al., 2005), peptides (Rachkov and Minoura, 2000), proteins (Burow and Minoura, 1996), antibodies (Vlatakis et al., 1993; Lerner et al., 1991) and double-stranded DNA (Slinchenko et al., 2004; Ogiso et al., 2007).

The high selectivity and affinity of MIPs for the template molecule offers a promising approach to develop a new generation of biosensors including sequence-specific DNA biosensors. Compared to other types of biosensors, which use biologically active molecules such as single-stranded DNA (ssDNA) immobilized onto the electrode surface as sensing elements, biosensors based on MIPs offer three advantages: (1) high affinity and selectivity to the imprinted template (i.e., the target molecules); (2) superior stability compared with those using natural biomolecules in the biosensor structure; and (3) ease of fabrication and adaptation for various types of biosensors (Mosbach and Ramstrom, 1996; Wulff, 1986; Nicholls et al., 1995).

To the best of our knowledge, this is the first report of a sequence-specific molecularly imprinted amperometric ssODN biosensor. The sequence-specific MIP electrode was prepared by electropolymerisation using a 17-mer single-stranded oligodeoxyribonucleotides (ss-ODN) as the template and *o*-phenylenediamine as the functional monomer. The 17-mer ss-ODN template used for this study is associated with the point mutation of human prostate cancer susceptibility gene *p53*. The clinical relevance of this research relates to the development of a biomimetic DNA biosensor, which would aid in the clinical diagnosis of this particular condition and as a model for other especially for genetic and infectious diseases.

2. Experimental

2.1. Materials

o-Phenylenediamine (Sigma, 98%), acetic acid (Sigma–Aldrich, ACS reagent, ≥99.7%), and sodium acetate (Sigma–Aldrich, ReagentPlus®, ≥99.0%) were used without further purification. All supplementary chemicals were of analytical grade and solutions were prepared using sterilised Milli-Q water (18.2 Ω/cm^2). Indium-tin-oxide (ITO) coated glass (Balzers) of 0.1 cm^2 sheets with a resistance of 15 Ω/cm^2 were used as substrates for the electro-deposition of poly(*o*-phenylenediamine) (PoPD) and ss-ODN imprinted PoPD electrodes.

For this study, we imprinted a 17-mer ss-ODN from p53 gene with a point mutation at codon 223. It is reported that point mutation occurring at codon 223 from CCT to C**T**T is associated with human prostate cancer (Isaacs et al., 1991). This mutated 17-mer ss-ODN was used both as the template during the preparation of the ss-ODN imprinted electrode and as the target during the analysis of the DNA biosensor analysis. Further, the specificity and/or selectivity of the ss-ODN imprinted biosensor were monitored under same conditions using the corresponding wild-type ss-ODN (i.e., the analogous ss-ODN) having only a single mismatch of the target. The ss-ODNs were purchased from Operon Biotechnologies Inc., USA.

Template ss-ODN (M_w 5257.48): 5′-TGAGCCGC**T**TGAGGTTG-3′
Target ss-ODN (M_w 5257.48): 5′-TGAGCCGC**T**TGAGGTTG-3′
Analogous ss-ODN (M_w 5242.45): 5′-TGAGCCGC**C**TGAGGTTG-3′

2.2. Fabrication of molecularly imprinted polymer (MIP) and non-imprinted polymer (NIP) electrodes

MIP electrodes were electrochemically synthesised (i.e., using cyclic voltammetry, CV) from a solution containing 5 mM *o*-phenylenediamine and 20 μM template ss-ODN in acetate buffer of pH 5.2, using a three-electrode assembly with the ITO glass as a working electrode, platinum as a counter electrode, and Ag/AgCl as a reference electrode at potentials ranging from 0.2 to 0.8 V and a scan rate of 50 mV s^{-1}. After polymerisation, the resulting ss-ODN/PoPD/ITO electrode was washed with sterilised ethanol-water (10:2, v/v) solution containing 0.1 M NaOH for 45 min followed by washing with Milli-Q water in order to remove the template ss-ODN molecules and to obtain the MIP/ITO electrode (Fig. 1A). The NIP/ITO electrode was synthesised under the same conditions as the MIP/ITO electrode except that no template ss-ODN was used. The MIP/ITO and NIP/ITO electrodes were dried under a nitrogen flow and stored at room temperature.

2.3. Amperometric recognition

The electrochemical detection was performed by CV with a three-electrode cell configuration comprising Ag/AgCl as a reference electrode, platinum as a counter electrode, and MIP/ITO as a working electrode in a 10 mM PBS of pH 7.4 containing 1 mM $Fe(CN)_6^{3-/4-}$ and 0.1 mM KCl at 50 mV s^{-1} scan rate. In the sequence-specific genetic recognition experiments, the MIP/ITO electrode was immersed in an electrochemical cell containing target ss-ODN (Fig. 1B). The concentration of target ss-ODN was varied in the range 0.01–300 fM. The biosensor interference study was performed by a subsequent addition of the analogous ss-ODN with a concentration ranging from 10 to 100 fM, in the presence of 200 fM target ss-ODN.

2.4. Dynamic binding interaction study

The binding behaviour of template ss-ODN onto the MIP/ITO electrode was measured using dynamic adsorbing-desorbing cyclic voltammetry (DCV) with a three-electrode configuration. The pre-adsorbed MIP/ITO electrode with 200 fM target ss-ODN was used as working electrode. The counter and reference electrode was platinum and Ag/AgCl, respectively. The electrolyte was phosphate buffer saline, pH 7.4 containing 1 mM $Fe(CN)_6^{3-/4-}$ and 0.1 mM KCl. The adsorption-desorption equilibrium of the target ss-ODN molecules on the MIP/ITO electrode were observed using DCV at a scanning rate of 50 mV s^{-1} up to 30 cycles.

2.5. Characterisation

All electrochemical measurements were carried out using a ALS/HCH 852CB potentiostat unit with three electrodes in buffer solution at fixed pH. The working electrodes were ITO, MIP/ITO or NIP/ITO whereas platinum and Ag/AgCl were used as the counter and reference electrode, respectively. FTIR spectra of the electrodes were recorded on a Galaxy series-3000 spectrophotometer using ATI-Mattson Quantum Infrared Microscope™. Further, the surface morphology of the electrodes was performed with a Hitachi S-4800 field emission scanning electron microscope (FESEM) operated at 5 kV. The specimens were sputter-coated with a thin layer of iridium (~5 nm) prior to examination. A 10 mM phosphate buffer saline (PBS) of pH 7.4 containing 1 mM $Fe(CN)_6^{3-/4-}$ and 0.1 mM KCl was

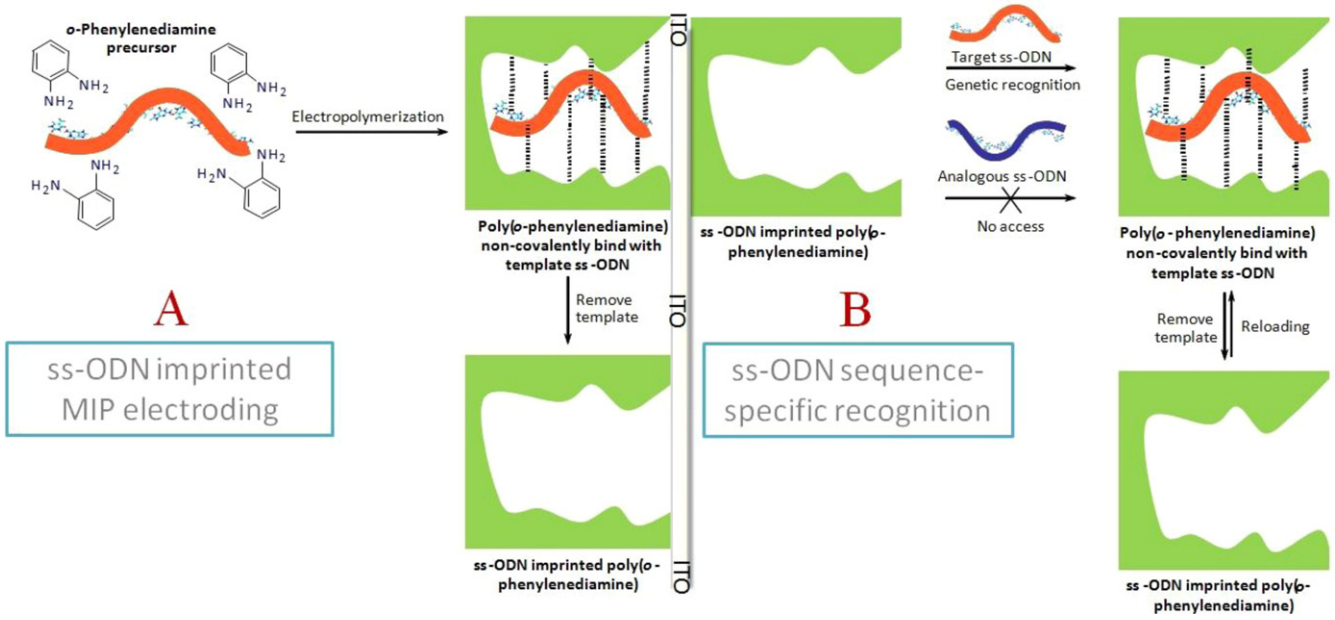

Fig. 1. (A) Electrochemical preparation of ss-ODN imprinted MIP electrode and (B) re-usable biosensor to recognise sequence-specific ss-ODN.

used as a redox electrolytic mediator for MIP genosensor study. All measurements were carried out at 20 ±2 °C.

3. Results and discussion

3.1. Preparation and characterisation of electrodes

The NIP/ITO electrode was prepared using electropolymerisation of *o*-phenylenediamine onto an ITO coated glass substrate, while the template ss-ODN/PoPD/ITO electrode was formed by adding the template ss-ODN together with the *o*-phenylenediamine during electropolymerisation. The MIP/ITO electrode was subsequently obtained by washing out of the template ss-ODN molecules from the template ss-ODN/PoPD/ITO electrode using sterilised ethanol-water (10:2, v/v) solution containing 0.1 M NaOH for 45 min followed by washing with Milli-Q water. The representative cyclic voltammograms of NIP/ITO and template ss-ODN/PoPD/ITO during electropolymerisation; and MIP/ITO electrodes after three successive washings are shown in Fig. 2. Fig. 2A shows that the NIP/ITO electrode was formed by progressively depositing the moderately non-conducting PoPD film onto the ITO surface with an increasing number of CV scans, resulting in a suppression of the voltammetric response. Since *o*-phenylenediamine monomer has $-NH_2$ (I) and $-NH_2$ (II), both of which can be available for electropolymerisation via dehydrogenation of available amino groups (Palmisano et al., 1995), the oxidation peak obtained in the first cycle might be assigned to the easily oxidisable amine group of the monomer. The cyclic voltammogram for the template ss—ODN/PoPD/ITO electrode was slightly different from those of the NIP/ITO electrode measured under the same conditions. As shown in Fig. 2B, current peak of template ss-ODN/PoPD/ITO electrode is appeared to be 2.16 times higher than NIP/ITO electrode in the presence of template ss-ODN within the potential range of 0.2–0.8 V at final CV cycle. The peak current decreased significantly with continuous CV scans. These observations suggested that the moderately non-conducting PoPD was deposited together with template ss-ODN onto the electrode surface and also deposition of template ss-ODN-PoPD increased with the number of scans. The peaks of the template ss-ODN-PoPD/ITO electrode might be attributed to the ionic alteration on the electrode collectively in the presence of template ss-ODN zwitterions (Feng et al., 2004).

Moreover, the peak current of the template ss-ODN-PoPD/ITO electrode decreased significantly with an increasing number of CV scans, indicating that both the template ss-ODN and accessible PoPD progressively deposited onto the ITO surface. PoPD and the zwitterion species of the template ss-ODN formed strong electrostatic interactions (i.e., between the two most nearest nitrogen or nitrogen and oxygen atoms with the hydrogen atom of neighbouring molecules) (Tiwari et al., 2008). Thus, during the process of electropolymerising *o*-phenylenediamine in the presence of template ss-ODN, the head-to-head and head-to-tail coupled moieties may meet. The nitrogen and/or oxygen atoms situated at different chemical environments in the coupled moieties could presumably provide the electrocatalytic effect for the imprinting of template. After the electropolymerisation, the template ss-ODN/PoPD/ITO electrode was washed with sterilised ethanol-water (10:2, v/v) solution containing 0.1 M NaOH followed by washing with Milli-Q water to remove the template ss-ODN molecules and to produce the MIP electrode. In other words, the ss-ODN imprinted PoPD/ITO electrode was prepared via two steps: (1) electropolymerisation of *o*-phenylenediamine monomer in the presence of ss-ODN templates; and (2) removal of the template ss-ODN. The cyclic voltammogram of the MIP/ITO electrode was found to be comparable redox peaks of $Fe(CN)_6^{3-/4-}$ after immersing the imprinted electrode in sterilised ethanol-water (10:2, v/v) solution containing 0.1 M NaOH for 45 min followed by three successive washing with Milli-Q water (Fig. 2C) indicating that the template ss-ODN was completely removed from the MIP/ITO electrode.

The electrochemical response of a thicker PoPD electrode may slow down the diffusion of the template ss-ODN, thereby reducing the response kinetics of the biosensor. Thus, forming a thin PoPD film on the electrode surface can improve the sensitivity of the sensor (Kriz et al., 1997). It was found that the thickness of the PoPD film formed by electropolymerisation can be controlled by adjusting the scan rate and the number of CV cycles at a specific *o*-phenylenediamine concentration. The optimum template incorporation with the PoPD film was observed with thirty CV scans at 50 mV s^{-1}.

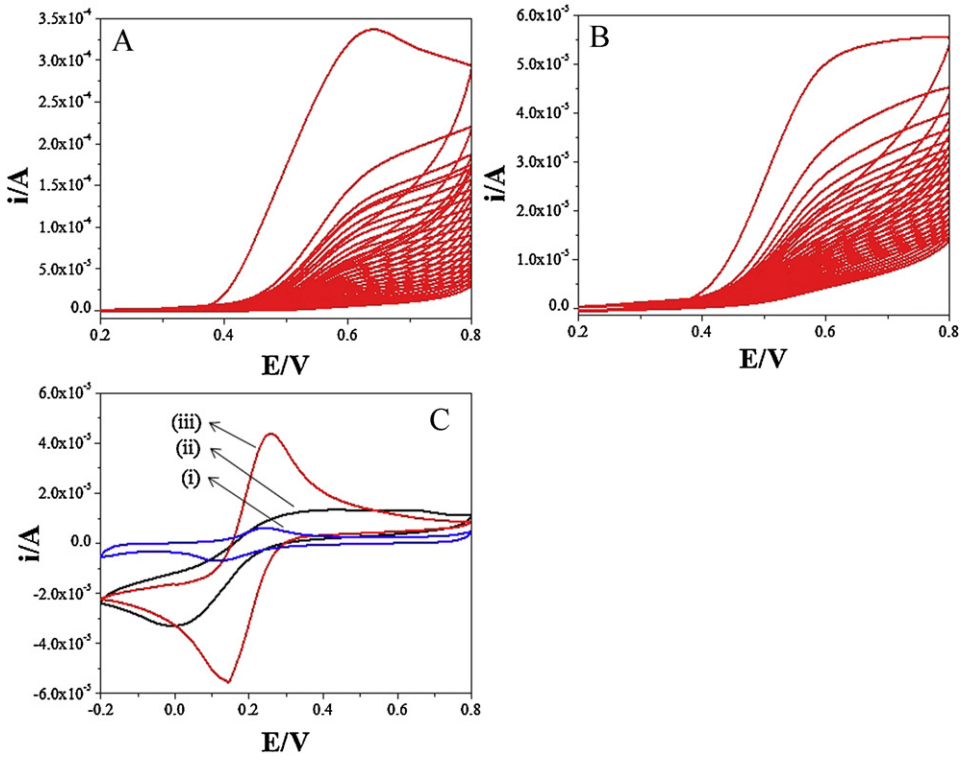

Fig. 2. Cyclic voltammograms of the (A) NIP/ITO, (B) template ss-ODN/PoPD/ITO in the acetate buffer of pH 5.2 at 50 mV s^{-1} scan rate vs. Ag/AgCl and 30 number of scans; and (C) MIP/ITO electrodes obtained after washing with sterilised ethanol-water (10:2, v/v) solution containing 0.1 M NaOH for 45 min followed by successive washing (i)–(iii) with Milli-Q water in a 10 mM PBS of pH 7.4 containing 1 mM $Fe(CN)_6^{3-/4-}$ and 0.1 mM KCl at 50 mV s^{-1} scan rate vs. Ag/AgCl.

Fig. 3 presents the FTIR spectra of the (A) ss-ODN/PoPD/ITO electrode, (B) MIP/ITO electrode, and (C) NIP/ITO electrode. The FTIR spectrum of the template ss-ODN/PoPD/ITO electrode showed peaks broadening at (1) 1228 cm^{-1} (phosphate vibration accredited to the phosphate backbone of the template ss-ODN); (2) 3108–3356 cm^{-1} (N—H stretching vibration); and (3) 1631–1669 cm^{-1} (amide vibrations), the higher frequency range may be attributed to a closer alignment of the template ss-ODN to the PoPD matrix due to the stronger intermolecular or interdomain hydrogen bonds (Tiwari and Gong, 2009). The FTIR spectra of the template ss-ODN/PoPD/ITO electrode confirmed the close electrostatic interaction between the template ss-ODN and the PoPD networks. After being washed with sterilised ethanol-water containing NaOH followed by washing with Milli-Q water, the resulting MIP/ITO electrode showed a similar FTIR spectrum as that of NIP/ITO. Namely, the MIP/ITO and NIP/ITO electrodes exhibited similar PoPD absorption bands within the range of 500–4000 cm^{-1} as reported in the literature (Lin and Zhang, 1996). Thus, the FTIR spectra confirmed the complete removal of the template ss-ODN from the template ss-ODN/PoPD/ITO electrode.

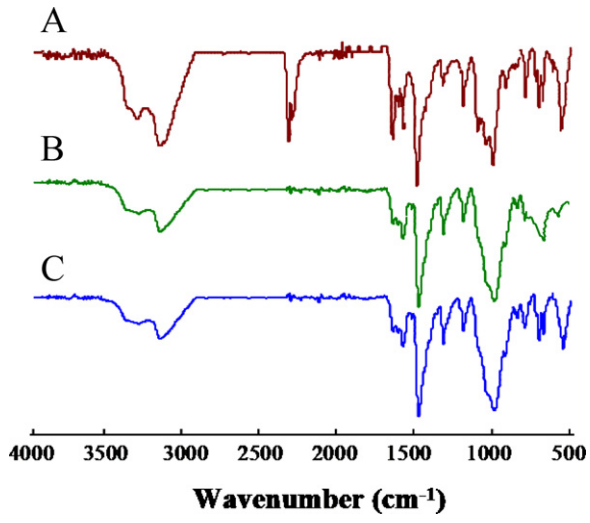

Fig. 3. FTIR spectra of the (A) template ss-ODN/PoPD/ITO, (B) MIP/ITO, and (C) NIP/ITO electrodes.

The surface morphology of the electrodes was observed with FE-SEM as shown in Fig. 4. The NIP/ITO electrode exhibited a relatively smooth and condensed topology (Fig. 4A), while the MIP/ITO electrode showed a rough and porous topology (Fig. 4B), which may be attributed to the imprinted ss-ODN structures present in the MIP/ITO electrode.

3.2. Amperometric recognition

The binding behaviour of the MIP/ITO electrode to target ss-ODN was studied via CV using target ss-ODN ranging from 300 to 0.01 fM in a 10 mM PBS of pH 7.4 containing 1 mM $Fe(CN)_6^{3-/4-}$ and 0.1 mM KCl at 50 mV s^{-1} scan rate vs. Ag/AgCl. Fig. 5A presents the CV diagrams of two MIP/ITO electrodes (i.e., one at lower concentration and one at higher concentration). The binding of target ss-ODN with the MIP/ITO electrode resulted in a positive potential at 0.09 V, indicating a strong interaction between the MIP/ITO electrode and the imprint species.

Fig. 5B shows the steady-state Δ current dependence calibration curve for the target ss-ODN concentration ranging from 0.01 to 300 fM. An amperometric linear response of Δi ($r^2 = 0.998$) was observed with the successive addition of target ss-ODN to the electrochemical cell under a constant stirring of 150 rpm at 2-min intervals. The electrode responded within 14 s to the change of target ss-ODN concentration. The interference effect of the analogous ss-ODN on the amperometric responses of the biosensor

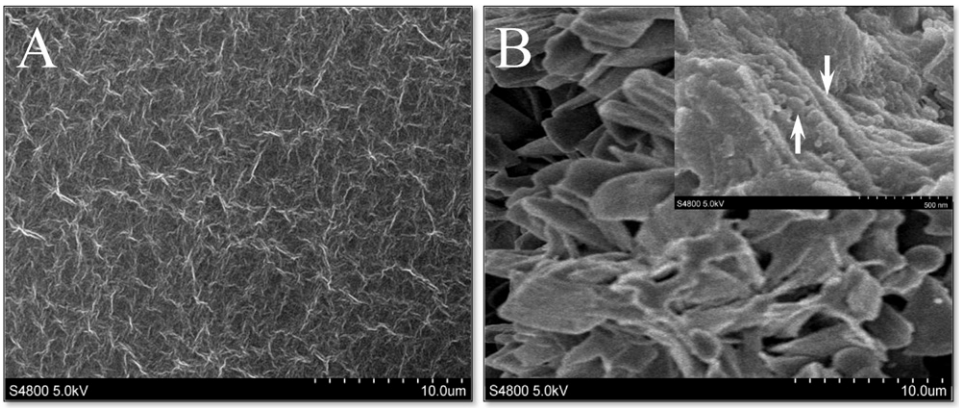

Fig. 4. SEM images of the (A) NIP/ITO and (B) MIP/ITO electrodes.

employing the MIP/ITO electrode was studied in the presence of 200 fM target ss-ODN. The effect of the analogous ss-ODN was investigated by measuring the amperometric response of the MIP/ITO biosensor with the successive addition of analogous ss-ODN at a concentration ranging from 10 to 100 fM. It was observed that the MIP/ITO biosensor had a relative error of less than ±4.65% with the addition of analogous ss-ODN. These results suggested that the prepared biosensor with the MIP/ITO electrode could detect sequence-specific ss-ODN with negligible interferences from the analogous ss-ODN. Thus, the DNA biosensor based on ss-ODN imprinted PoPD/ITO electrode demonstarted precise recognition with the target ss-ODN.

The current sensitivity of the MIP/ITO electrode towards target ss-ODN concentrations was 0.62 μA/fM. The analogous ss-ODN showed about ±4.97% current response with the MIP/ITO electrode. In a control experiment, the NIP/ITO electrodes showed an approximately similar type of amperometric response with the target and analogous ss-ODN when 10–200 fM of target or analogous ss-ODN was added successively to the NIP/ITO biosensor. Thus, fabricated MIP/ITO electrode is precisely detect target ss-ODN.

3.3. Kinetics and stability

The stability of the MIP/ITO electrode was studied by measuring the current at different temperatures ranging from 20 to 35 °C in the presence of 200 fM target ss-ODN. It was observed that the adsorption/binding reaction rate of target ss-ODN onto the MIP/ITO electrode increased with the temperature up to 30 °C and the optimum temperature range was between 25 and 30 °C. This observation may be attributed to the increased kinetic movement

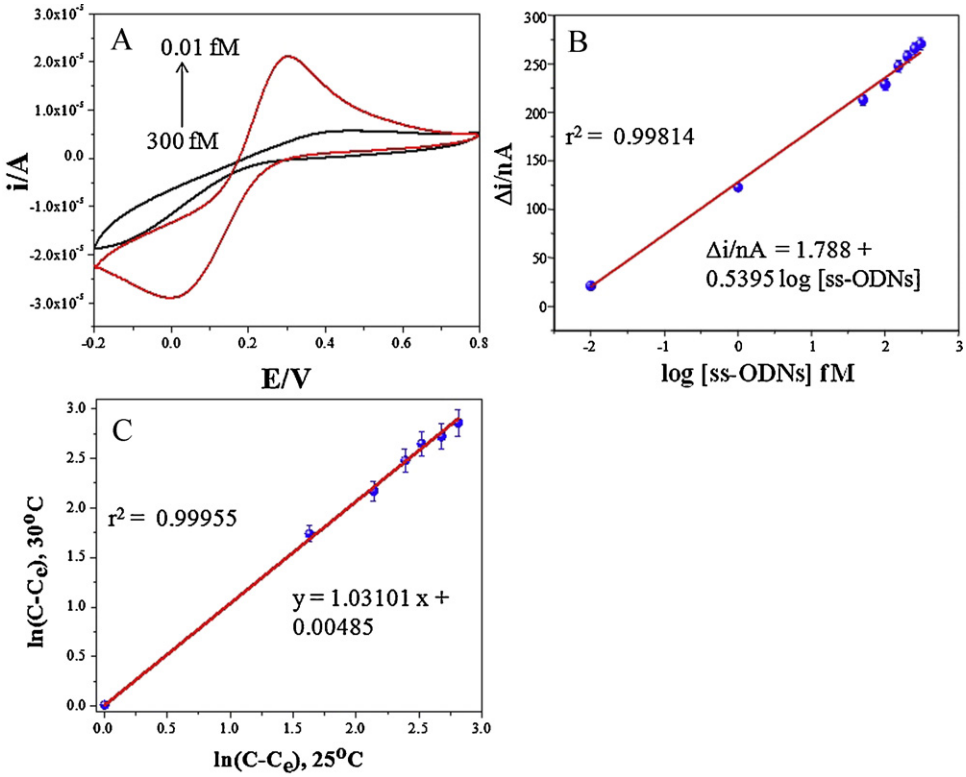

Fig. 5. (A) The cyclic voltammogram of the MIP/ITO electrode in the presence of target ss-ODN, (B) the steady-state Δ current response of the MIP/ITO biosensor as a function of the logarithm of molar concentration of the target ss-ODN, and (C) the relative adsorption of the target ss-ODN onto the MIP/ITO electrode at a concentration ranging from 0.01 to 300 fM at 25 and 30 °C. Values of (B) and (C) are mean ± SE; %SD = 4.61; $n = 5$. Working conditions: supporting electrolyte – 10 mM PBS of pH 7.4 containing 1.0 mM $Fe(CN)_6^{3-/4-}$ and 0.1 mM KCl at 50 mV s^{-1} scan rate vs. Ag/AgCl.

of the target ss-ODN molecules onto the electrode surface. Correlating the adsorption concentration of the target ss-ODN onto the MIP/ITO electrode at different temperature based on Eq. (1):

$$\ln(C - C_e)_H = A_r \cdot \ln(C - C_e)_L \quad (1)$$

where C and C_e stand for the taken and equilibrium concentrations of the target ss-ODN onto the MIP/ITO electrode, respectively. The subscripts 'L' and 'H' represent the relatively low temperature and high temperature, respectively. A_r is a constant that reflects the relative adsorption rate. Using Eq. (1), the effect of temperature on the relative adsorption of the target ss-ODN onto the MIP/ITO electrode can be obtained by plotting $\ln(C - C_e)_H$ vs. $\ln(C - C_e)_L$ (Srihari and Das, 2008). Fig. 5C illustrates a linear relationship of $\ln(C - C_e)$ at 30 °C vs. $\ln(C - C_e)$ at 25 °C and the relative specificity can be revealed from the slope (i.e., $A_r = 1.031$). Thus, at a higher temperature, the MIP/ITO electrode showed a higher adsorption/binding rate with the target ss-ODN ($A_r > 1$). The storage stability of the MIP/ITO electrode was amperometrically measured and a similar current response was obtained about twenty weeks at room temperature.

3.4. Reproducibility and accuracy

The lowest detection limit of the MIP/ITO electrode was 0.01 fM. The reproducibility of the response of the MIP/ITO electrode was investigated at a 200 fM target ss-ODN concentration. No significant decrease in current response was observed after at least 10 tests; thus, the imprinted electrode displayed good reproducibility. The relative standard deviation was determined by five successive measurements of a 200 fM target ss-ODN using the same MIP/ITO electrode (i.e., used each time after washing) and was found to be ±5.28%. In a series of ten target ss-ODN sensing measurements, with ten different MIP/ITO electrodes, a relative standard deviation of ±4.63% was obtained for the individual current response of the same sample (i.e., 200 fM target ss-ODN). Thus, an excellent reproducibility was observed with this biosensor, which can be attributed to the efficient bonding of the target ss-ODN with the MIP/ITO electrodes.

4. Conclusion

A new type of molecularly imprinted ss-DNA biosensor was successfully fabricated and evaluated. The ss-DNA biosensor was fabricated by an electropolymerisation process on an indium-tin oxide coated glass substrate using single-stranded oligodeoxyribonucleotides (ss-ODN) as the template and *o*-phenylenediamine as the functional monomer. The ss-DNA biosensor showed a linear Δ current response to the target ss-ODN concentration ranging from 0.01 to 300 fM and it exhibited a sensitivity of 0.62 μA/fM, with a response time of 14 s. The relatively low analogous ss-ODN interference effect of SD = ±4.97% indicates that the MIP/ITO electrode surface had a high affinity for the target ss-ODN. This new type of ss-ODN biosensor has demonstrated good performance including a long shelf life, higher sensitivity, wide analytical range and fast response time.

Acknowledgements

The authors thank Linköping University, Sweden and National Institute for Materials Science, Japan for providing facilities. We also wish to thank the European Commission (PIIF-GA-2009-254955), IGEN, JSPS, JST-CREST and MEXT for generous financial support to carry out this research.

References

Ansell, R.J., Kriz, D., Mosbach, K., 1996. Curr. Opin. Biotechnol. 7, 89–94.
Bruce, A., Johnson, A., Lewis, J., Raff, M., Roberts, K., Walters, P., 2002. Molecular Biology of the Cell, 4th edition. Garland Science, New York.
Burow, M., Minoura, N., 1996. Biochem. Biophys. Res. Commun. 227, 419–422.
Haupt, K., Mosbach, K., 2000. Chem. Rev. 100, 2495–2504.
Feng, L., Liu, Y., Tan, Y., Hu, J., 2004. Biosens. Bioelectron. 19, 1513–1519.
Isaacs, W.B., Carter, B.S., Ewing, C.M., 1991. Cancer Res. 51, 4716–4720.
Kerman, K., Kobayashi, M., Tamiya, E., 2004. Meas. Sci. Technol. 15, R1–R11.
Kriz, D., Ramstrom, O., Mosbach, K., 1997. Anal. Chem. 69, 345A–349A.
Lerner, R.A., Benkovic, S.J., Schultz, P.G., 1991. Science, 659–667.
Lin, X., Zhang, H., 1996. Electrochim. Acta 41, 2019–2024.
Liu, B., Bazan, G.C., 2005. PNAS 102, 589–593.
Merkoci, A., Alegret, S., 2002. Trends Anal. Chem. 21, 717–725.
Mosbach, K., 1994. Trends Biochem. Sci. 19, 9–14.
Mosbach, K., Ramstrom, O., 1996. Nat. Biotechnol. 14, 163–170.
Nicholls, I.A., Ramström, O., Mosbach, K., 1995. J. Chromatogr. A 691, 349–353.
Ogiso, M., Minoura, N., Shinbo, T., Shimizu, T., 2007. Biosens. Bioelectron. 22, 1974–1981.
Palmisano, F., Guerrieri, A., Quinto, M., Zambonin, P.G., 1995. Anal. Chem. 67, 1005–1009.
Parmpi, P., Kofinas, P., 2004. Biomaterials 25, 1969–1973.
Piletsky, S.A., Alcock, S., Turner, A.P.F., 2001. Trends Biotechnol. 19, 9–12.
Rachkov, A., Minoura, N., 2000. J. Chromatogr. A 889, 111–118.
Ramanaviciene, A., Ramanavicius, A., 2004. Biosens. Bioelectron. 20, 1076–1082.
Slinchenko, O., Rachkov, A., Miyachi, H., Ogiso, M., Minoura, N., 2004. Biosens. Bioelectron. 20, 1091–1097.
Shiomi, T., Matsui, M., Mizukami, F., Sakaguchi, K., 2005. Biomaterials 26, 5564–5571.
Srihari, V., Das, A., 2008. Desalination 225, 220–234.
Tiwari, A., Sen, V., Dhakate, S.R., Mishra, A.P., Singh, V., 2008. Polym. Adv. Technol. 19, 909–914.
Tiwari, A., Gong, S., 2009. Talanta 77, 1217–1222.
Vlatakis, G., Andersson, L.I., Müller, R., Mosbach, K., 1993. Nature 361, 645–647.
Wang, J., 2000. Nucleic Acids Res. 28, 3011–3016.
Whitcombe, M.J., Rodriguez, M.E., Villar, P., Vulfson, E.N., 1995. J. Am. Chem. Soc. 117, 7105–7111.
Wizeman, W.J., Kofinas, P., 2001. Biomaterials 22, 1485–1491.
Wolfram, S., 1984. Principles of Nucleic Acid Structure. Springer-Verlag, New York.
Wulff, G., 1986. In: Ford, W.T. (Ed.), Polymeric Reagents and Catalysts, vol. 308. American Chemical Society, Washington, DC, pp. 186–230.